

He⁴ State Equation Below 0.8 K

V. Arp¹

Received November 19, 2004

This work develops the Helmholtz potential $A(\rho, T)$ for He⁴ below 0.8 K. Superfluid terms, related to temperature and momentum gradients, are neglected with negligible loss of accuracy in the derived state properties (specific heats, first sound velocity, expansivity, compressibility, etc.). Retained terms are directly related to a bulk fluid compressibility plus phonon and roton excitations in this quantum fluid. The bulk fluid compressibility is found from the empirical equation $c_1^3 \approx c_{10}^3 + b; P$, where c_1 is the velocity of first sound, P is the pressure, and c_{10} and b are constants; this empirical equation is found to apply also to other helium temperature ranges and to other fluids. The phonon excitations lead to a single temperature-dependent term in $A(\rho, T)$ up to 0.3 K, with only two more terms added up to 0.8 K. The roton potential, negligible below about 0.3 K, is a single term first derived 60 years ago but little used in more recent work. The final $A(\rho, T)$ is shown to fit available experimental specific heat data to about $\pm 2\%$ or better. The magnitude of the pressure-independent Gruneisen parameter below 0.3 K is typical of highly compressed normal liquids. Extension of the equation above 0.8 K is hampered by lack of data between 0.8 and 1.2 K.

KEY WORDS: bulk fluid compressibility; Gruneisen parameter; helium II; helium-4; Helmholtz energy; phonons; rotons; sound velocity; specific heat; state equation.

1. INTRODUCTION

The basic approach in this work is to find an analytical expression for the Helmholtz energy, A , of He⁴ which is consistent with all measured state properties of the fluid. In the HeII range, nominally below 2.17 K, the Helmholtz energy is a function of density, temperature, and the velocity difference between superfluid and normal fluid components (in the

¹Cryodata, Inc., Boulder, Colorado, U.S.A. E-mail: varp@cryodata.com

two-fluid model [1]), or of density, temperature, temperature gradient, and momentum gradient (in the newer extended model [2]). However, in static fluid the density and temperature derivatives of the Helmholtz energy are essentially independent of these unique superfluid gradient terms, especially below 0.8 K. In this work, the Helmholtz energy is assumed to depend only on density and temperature, such that pressure, entropy, specific heats, expansivity, compressibility, etc., are determined by classical fluid-state derivatives.

The Helmholtz potential $A(T)$ for the high frequency fluid excitations, unique to He^4 , was first derived by Landau [3, 4] in the 1940s, based somewhat intuitively on quantized hydrodynamics and an imprecisely known energy gap in the elementary excitation spectrum. After neutron spectroscopy studies of the excitation spectrum became available in the 1960s and 1970s, Donnelly and coworkers [5] developed the thermodynamics and numerical calculation methods [6] leading directly from the measured excitation spectrum to extensive tabular data for both state and transport properties, often referenced yet today. Landau's Helmholtz roton function was not utilized in the Donnelly analysis. The upper temperature limit for the Donnelly data is about 0.1 K below the lambda line. Today, modest deviations between the Donnelly tabulations and some newer experimental data are acknowledged.

In 1980 McCarty [7] published a computer program state equation fitted to the Brooks and Donnelly tabular data [6], plus some newer data. The code is not referenced to Landau's Helmholtz function, nor is it separable into phonon and roton terms (low- and high-frequency terms) of the excitation spectrum. It is divided into three intervals, 0 to 0.8 K, 0.8 to 1.2 K, and 1.2 K to near the lambda line, with a selected mathematical state function but different constants used in each interval.

In this work, available He^4 data are re-examined to produce a Helmholtz energy equation $A(\rho, T)$ composed of separate compressed fluid, phonon and roton terms, utilizing Landau's Helmholtz function. The upper temperature limit is based on factors discussed below.

2. DATA SOURCES

Some data used in this work deserve special discussion. Phillips et al. [8] measured C_v along four isochores from about 0.1 K to above 1 K. Their experimental data points were never published [9], and their results exist today only in the form of four equations. The equations are stated to fit their individual isochore data with a precision of about 0.5%. The Phillips data discussed below were all generated from his published equations.

Greywall [10] measured C_v data along 11 isochores from 0.05 to 1.02 K (at saturation pressure) or to 0.84 K (at near-melting pressure) correlated with an in-depth theoretical analysis. His tabular experimental data are available from the American Physical Society (APS) archives. Later he published an erratum [11] in which he reported a small thermomolecular pressure correction error in the original data. In that erratum he published an equation which was a “satisfactory” fit to the corrected data. In this work, the original tabular data indeed led to some seemingly irreducible and localized fitting errors of up to several percent, but data generated from his erratum equation reduced the fitting errors to under 1%. My conclusion is that the APS archive data do not include the pressure measurement correction. Both sets of data have been considered here, out of interest, but little weight was given to his tabular data in the least-squares fitting process.

Donnelly and Barenghi [12] have published a comprehensive compilation of 19 thermodynamic properties of helium along the saturation line, collected from an extensive bibliography. The publication includes “recommended” values of parameters, based on spline computer fits to their collected data. In this work, their recommended values are referenced in some cases, without explicit reference to the prior publications on which their spline fit is based.

All of the input data used in this work were taken on the T58 temperature scale. The T90 scale [13] is the currently accepted international standard, but it is defined only between 1.2 and 5.0 K. In this work all temperatures were converted to the T76 scale, which is defined from 0.5 K to the critical temperature of 5.1953 K [14]. Where the T90 scale is defined, the T76 scale is almost identical to it (within about $\pm 50 \mu\text{K}$). Below 1.2 K, the T76 scale is based on theory which is valid down to 0 K even though the fitted equation terminates at 0.5 K. Below 0.8 K the correction from T58 to T76 is given to adequate precision by $T76 = T58 \times 1.0031$

3. TEMPERATURE-INDEPENDENT STATE TERMS

A baseline in this work includes the very precise measurements by Abraham et al. [15] of sound velocity, c_1 , as a function of pressure, P , from 0 to about the melting pressure (about 2.5 MPa). (Here c_1 refers to the ordinary sound velocity, an isentropic density wave, usually termed “first sound” in HeII studies. It differs from “second sound”, a temperature wave, uniquely found in HeII above about 1 K.) Their measurements were made along two isotherms, one at or below 0.1 K, and the other at 0.5 K. Data from the two isotherms agree to better than 0.1%, illustrating

a negligible temperature dependence. In this work, their 0.1 K data are accepted as representing the state properties at 0 K.

Maris [16] subsequently made the important observation that c_1^3 appears to be linear in P over all the measured range, as illustrated in Fig. 1. In mathematical test a small quadratic term is statistically significant although hardly visible in that figure. The equation,

$$c_1^3 = c_{10}^3 + b_1 P + b_2 P^2 \quad (1)$$

fits their data to very high precision, with the ratio $b_2 P / b_1 \approx 0.0035$ at maximum observed pressure. A separate discussion of the applicability of

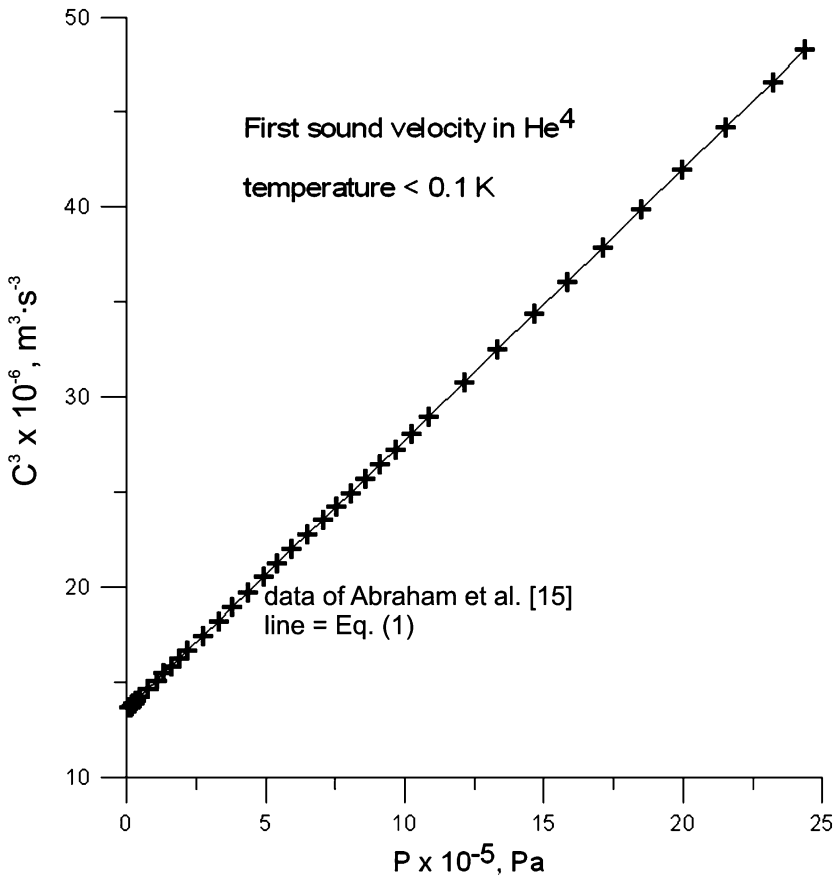


Fig. 1. (First sound velocity)³ as a function of pressure for temperature < 0.1 K. Detailed analysis discloses a very small but non-zero second derivative to this curve.

Eq. (1) to other fluids is found in Appendix A of this paper. In this work, I hypothesize that Eq. (1) is a property of the bulk fluid, independent of superfluid parameters and independent of temperature below 0.8 K.

For an ordinary fluid, in the absence of dispersion,

$$c_1^2 = \partial P / \partial \rho|_S \quad (2)$$

is a thermodynamic identity. In superfluid, however, the perturbation from the “second sound” mode reduces Eq. (2) to an approximation in the bulk fluid. Small corrections to Eq. (2), dependent on the velocity of second sound, have been discussed in terms of the two-fluid model [1], and are also available in the newer extended HeII theory [2]. These second-sound corrections are less than 0.1% for temperatures below 1 K, and they are neglected in this work.

At zero temperature, the entropy of HeII is zero for all pressures. At 0.1 K, the difference between isentropic and isothermal processes remains negligible, so that

$$c_1^2 = \partial P / \partial \rho|_T \quad (3)$$

is an excellent approximation for integration of the Fig. 1 data.

It should be noted that if the linearity of Fig. 1 is exact, i.e., if $b_2 = 0$ in Eq. (1), then that equation and Eq. (3) can be combined in an analytical integration to obtain the equation,

$$P = \sum a_i (\rho - \rho_0)^i, \quad i = 1 \text{ to } 3. \quad (4)$$

where $a_2^2 = 3a_1a_3$. The three a_i terms are simple algebraic functions of the two parameters c_{10} and b_1 . Abraham et al. [15] observed that only three terms seemed to be required in Eq. (4) to provide an accurate density-dependent state equation in the zero T limit. The constant of integration in Eq. (4) is taken as $\rho_0 = 145.1397 \text{ kg} \cdot \text{m}^{-3}$ [17].

There is no known physical law which says that the apparent linearity in Fig. 1 should be exact, however, and I choose to retain the non-zero b_2 in Eq. (1). In this case Eqs. (1) plus (3) cannot be analytically integrated, so that numerical integration is used to obtain $P(\rho)$, fitted to a revised Eq. (4) with $i = 1$ to 5. The final equation for the Helmholtz potential, consistent with Eq. (4), is

$$A_0(\rho) = -a_{00}/\rho + a_{01} \log(\rho) + a_{02}\rho + a_{03}\rho^2 + a_{04}\rho^3 + A_{00} \quad (5)$$

where A_{00} is chosen so that $A(\rho_0) = 0$. The constants are listed in Appendix B. Equation (5) can be differentiated to predict the pressure and isothermal compressibility and the isentropic compressibility in the low T

limit. The extrapolated sound velocity at $P = 0$ is $c_{10} = 238.28 \text{ m} \cdot \text{s}^{-1}$, agreeing well with the value of $238.30 \pm 0.13 \text{ m} \cdot \text{s}^{-1}$ deduced by Whitney and Chase [18] from a compilation of earlier measurements. The selected fit of Eq. (5) to (1) is valid to 3.2 MPa, which is an extrapolation beyond the maximum measured pressure of about 2.5 MPa. Such extrapolation seems reasonable as a working hypothesis in view of the high degree of linearity in Fig. 1. The extended range of Eq. (5) constants makes it a feasible equation for later use in a helium state equation fitted to pressures near that of the upper lambda point.

4. STATE EQUATION BELOW 0.3 K

Below about 0.3 K, only low-frequency excitations, or phonons, contribute to the thermodynamics, and the specific heat of the liquid is proportional to T^3 in this low temperature limit;

$$C_v = a(\rho)T^3. \quad (6)$$

The density-dependent factor, $a(\rho)$, can be determined simply from Fig. 2, which plots C_v/T^3 from both Phillips et al. [8] and Greywall [10,11] for all T in the range of 0.1 to 0.2 K as a function of ρ^k , with $k = -8.586$. The linearity in Fig. 2 is consistent with the simple state equation,

$$A(\rho, T) = A_0(\rho) + a_1 \rho^k T^4 \quad (7)$$

where $A_0(\rho)$ is Eq. (5), and a_1 is a numerical constant determined from the slope of the line in Fig. 2. At this point it is useful to recognize the (dimensionless) Gruneisen parameter, defined by

$$g = V \partial P / \partial U|_V = \partial P / \partial T|_V / (\rho C_V) \quad (8)$$

Differentiation shows that the constant k in Eq. (7) is equivalent to a density and temperature independent Gruneisen parameter $g = k/(-3) \approx 2.862$. Gruneisen parameter values for compressed monatomic or diatomic liquids at, e.g., $T/T_c \approx 0.7$ and densities near the melting line, are typically in the range of 1.5–3, although mildly temperature and pressure dependent. Measured by this parameter, the thermal term in Eq. (7) represents a highly compressed phonon fluid.

(Other thermodynamic definitions of the term “Gruneisen parameter” have been given in the literature [19]. The Eq. (7) definition is commonly used in the study of aerodynamic shocks. In some NIST fluid properties tabulations it was termed “energy derivative” and labeled with units.)

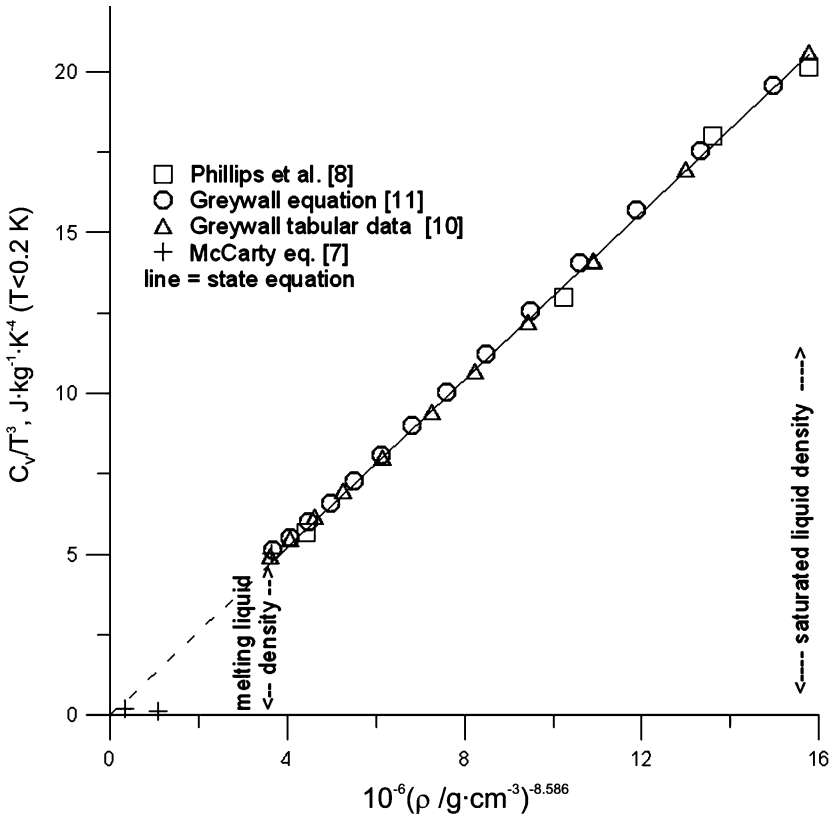


Fig. 2. C_v/T^3 as a function of $(\text{density})^{-8.586}$ for all measured temperatures ≤ 0.2 K. Symbols are experimental data points. The line is the fitted state equation. The dashed portion of the line has no physical meaning.

In extracting other thermodynamics from Eq. (7), it is useful also to recognize the thermodynamic identity,

$$C_P/C_V = \gamma = 1 + \alpha g \tag{9}$$

where α is the dimensionless thermal expansivity,

$$\alpha = (T/V) \partial V / \partial T |_P \tag{10}$$

Like the specific heat, the thermal expansion $(1/V) \partial V / \partial T |_P$ is proportional to T^3 in this range. Equation (7) is the state equation for helium below about 0.3 K.

5. EQUATION EXTENSION TO 0.8 K

Above about 0.3 K, high frequency roton states in the excitation spectrum begin contributing measurably to the thermodynamic properties, and higher-order terms in the phonon spectrum are also encountered.

In the 1940s, Landau [3, 4] developed the Helmholtz potential of roton states as

$$A_R = fVT^{1.5}e^{(-\Delta/T)} \quad (11)$$

where V is the specific volume and Δ is the energy gap (in kelvins, as written here) between the He^4 ground state and the minimum roton energy. The factor f includes an effective mass of the helium atom times fundamental constants, and so is treated in this work as an adjustable parameter, possibly a function of density. The energy gap Δ is known to decrease as the density increases.

Both Phillips et al. [8] and Greywall [11] used an equation for C_V which is derived directly from Eq. (11). Phillips et al. evaluated a unique Δ and f for each of their four isochores. Greywall included polynomial approximations for both Δ and (fV) as a function of ρ .

Phonon excitations above 0.3 K have been discussed in some detail by Greywall [10]. Along any isochore they are known to be described by a specific heat series;

$$C_v = aT^3 + cT^5 + dT^6 + eT^7 \dots \quad (12)$$

Phillips et al. obtained the best statistical fit to their data by including only the T^3 and T^5 terms. Greywall considered all of the listed terms in Eq. (12) over a slightly wider temperature range, but does not include the T^6 term in his final equation [11].

In the present work a number of plausible variations of Eqs. (11) and (12) have been tested. An analytical form for the decrease in Δ with increasing density (or pressure) is suggested by the equations of Maynard [1] for helium between 1.2 K and the lambda line. Using (P, T) coordinates, Maynard's Figs. 8 and 9 support his conclusion that both Δ and the superfluid density fraction ρ_s/ρ are uniquely determined by the single parameter $T/T_\lambda(P)$, where T_λ is the temperature at the lambda line. One can extrapolate from his work to conclude that, in our range below 0.8 K, Δ may be proportional to $T_\lambda(P)$, or perhaps the isochoric equivalent $T_\lambda(\rho)$. Marginal success was found with both of these trial equations, though clouded by some question as to the most accurate equation for $T_\lambda(P)$ or $T_\lambda(\rho)$. Also, the $T_\lambda(\rho)$ calculation is further clouded here by the 0.667% shift in saturated liquid density between $T=0$ and $T=2.17$ K.

An alternative equation for Δ is suggested by Fig. 20 of Greywall [10], which shows that Δ varies essentially linearly with pressure. Finally we assume

$$\Delta = \Delta_0 + m P_0(\rho) \quad (13)$$

where Δ_0 and m are least-squares fitted constants, and $P_0(\rho)$ is determined only from Eq. (5). Overall, the fit using Eq. (13) is significantly better and less ambiguous than using any proportionality to $T_\lambda(P)$ or $T_\lambda(\rho)$ as suggested in the paragraph above.

After trying various possible density dependences for the factor (fV), the best fit is obtained with f equal a constant (leaving just the factor V) in Eq. (11).

For the phonon contribution, a fully satisfactory solution is found using only the T^3 and T^5 terms of Eq. (12). It turns out that the two-term expression,

$$c(\rho)T^5 = 30(c_0 + c_k\rho^k)T^5 \quad (14)$$

fits the data as well as do other possible expressions with larger numbers of terms. Here c_0 , c_k , and k are constants, with 30 as an arbitrary numerical factor. Least-squares fitted values of k generally were in the range of -8 to -9 , and negligible fitting accuracy is lost by assuming k in Eq. (14) is the same numerical value as k in Eq. (7).

The coefficient $c(\rho)$ in Eq. (14) has caused discussions among theoreticians because it is negative at low pressure and positive at high pressure, with concomitant implications for qualitative changes in phonon scattering mechanisms as a function of pressure or density. The present work seems to relate that change to the presence of a single specific heat term $c_0 T^5$ added to the ($\rho^k T^3$ plus $\rho^k T^5$) hierarchy of terms.

The final state equation below 0.8 K is then

$$A(\rho, T) = A_0(\rho) + a_1\rho^k T^4 + (c_0 + c_k\rho^k)T^6 + fT^{1.5}e^{(-\Delta/T)}/\rho \quad (15)$$

With $A_0(\rho)$ and k determined in previous steps, only six least-squares fitted constants remain to be determined. Fitted constants are listed in Appendix B.

6. LEAST-SQUARES RESULTS AND DISCUSSION

C_v data are most important in determining the thermal coefficients. Because most C_v input data were from a collection of fitted equations rather than individual data points, the use of statistical measures of fit

may not be fully applicable. Qualitative measures of fit can be deduced from Figs. 2–4 for three different isotherms, and Fig. 3 along the saturation line. Greywall's "equation" data [11] were given the dominant statistical weight in the least-squares process.

Probably the most precise experimental value of Δ_0 , from neutron spectroscopy [20], is $\Delta_0 = 8.618$ K. Our least-squares fitted value is $\Delta_0 = 8.602$ K, in very good agreement. Least-squares fitting deviations between the final equation and 42 C_v data points from Phillips et al. [8] have an rms deviation of 1.54% with a maximum deviation of 2.65%. These deviations are somewhat larger than the estimated precision of Phillips et al.,

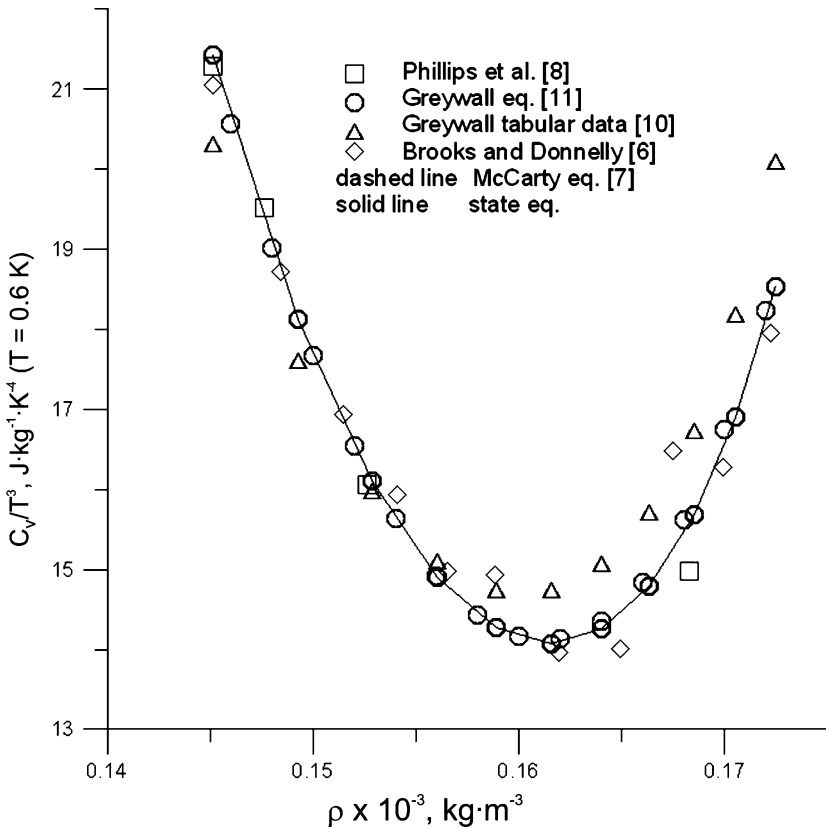


Fig. 3. Percent deviations between measured or predicted C_v and the state equation C_v as a function of temperature, at pressures along the saturation line. The two predicted correlations (Refs. 6 and 7) were based largely on preliminary data, now acknowledged to be of uncertain accuracy.

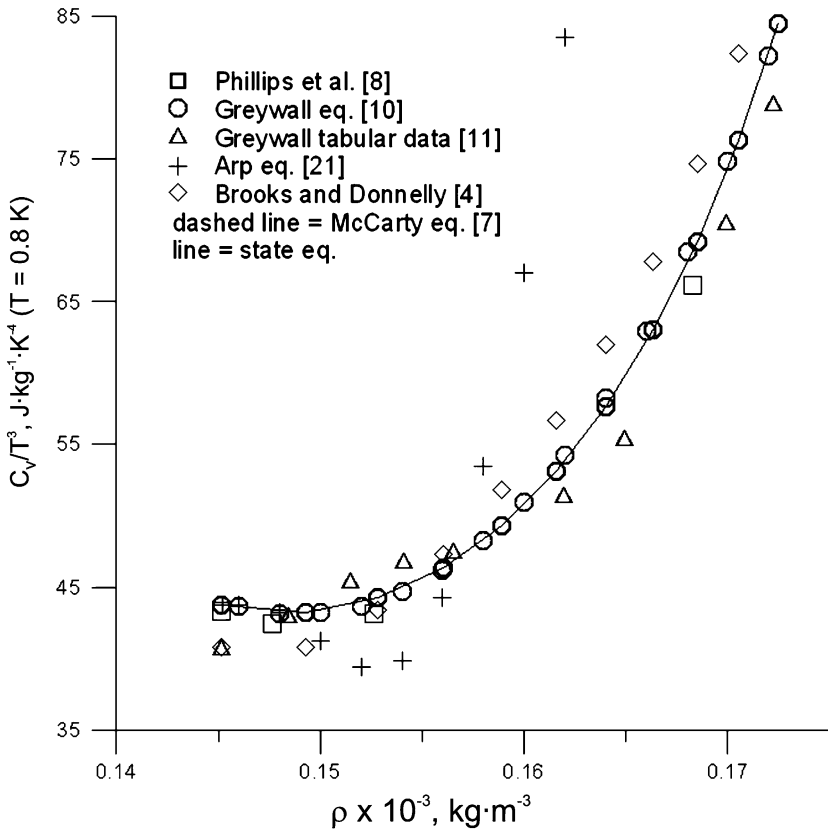


Fig. 4. C_v/T^3 as a function of density for all data with $T \approx 0.6$ K. Symbols are experimental data points. The line is the fitted state equation, which is weighted towards the “Greywall eq.” (Ref.11) experimental data.

and appear to be related to density measurement differences. 210 C_v data points from the Greywall equation [11] have an rms deviation of 0.42% with a maximum deviation of 1.68% (Fig. 4). Deviations of the (older) C_v data [6, 7] are in the 1 to 2% range below about 0.5 K, rising to the 10% range at higher temperatures; these data were given a zero least-squares weight. 16 “recommended” C_{sat} [12] data points along the saturation line have an rms deviation of 1.17%. It is realistic to accept that both the Donnelly [6] and McCarty [7] numerical results are based upon more

limited data and are not as accurate as the present state equation. Overall, it is my judgment that the state-equation specific heats are conservatively accurate to about 2%.

An important lesson is to be learned from the poor fit of Arp [21] data in Fig. 5. Those data points were calculated from a Helmholtz equation which is a good fit to *PVT*, first- and second-sound, specific-heat, and other data from 1.2 K to the lambda line. The equation was extended from 1.2 K down to 0.8 K fitting just saturation properties, plus available higher-pressure *PVT* and first sound velocity data. The present conclusion is that the *PVT* and first-sound velocity fits were not adequate to maintain calculated specific-heat accuracy at 0.8 K. High-pressure, experimental specific-heat data for this fluid are required for such a quasi-extrapolation.

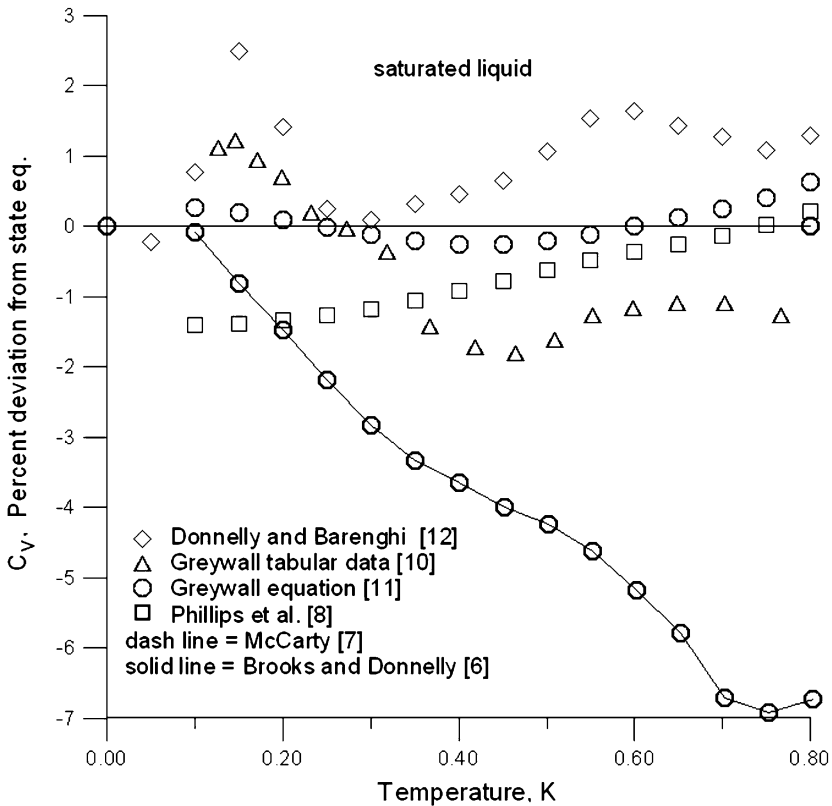


Fig. 5. C_v/T^3 as a function of density for all data with $T \approx 0.8$ K. Symbols are experimental data points. The line is the fitted state equation, which is weighted towards the "Greywall eq." (Ref. 11) experimental data.

Grilly and Mills [22] have measured PVT and derivatives along the melting line for $0.3\text{ K} \geq T \geq 2.0\text{ K}$. In several tests among our ongoing studies of helium properties near the lambda line (to be published), we have tentatively concluded that the tabulated densities of Grilly and Mills should be reduced by roughly 0.15–0.20% in order to obtain an overall better fit with measured lambda line properties. In the present work we find that a density reduction of 0.27% obtains state equation agreement with their tabulated pressures to better than 0.02%. I choose to identify the 0.27% density shift as an output of this work rather than trying to adjust the precisely determined coefficients of Eq. (5) or (14) to fit their unadjusted PVT data. Density shifts or errors of this magnitude are not unexpected in fluid properties correlations.

The compressibility data of Grilly and Mills below 0.8 K were obtained from small differences in pressure gage readings and disagree with Eq. (5) by about 3.6%. They were given zero weight in least-squares data fitting. The measured values of dV/dT of Grilly and Mills are near the lower limits of their resolution and are tabulated only to 1 or 2 significant figures in our temperature range. The deviation of their data from the fitted curve (translated into dP/dT , using dP/dV from Eq. (5)) is shown in Fig. 6. I judge this to be satisfactory agreement.

Niemela and Donnelly [17] list equations summarizing calculated $\rho_{\text{sat}}(T)$ and the isobaric expansivity. The temperature variation of these quantities is essentially determined by the density-dependent specific-heat data. A quantity of interest is the total density change from 0 to 0.8 K, since this is one stage in calculating the density at 0 K from their nearest directly measured density at 1.344 K. Their equations give $\Delta\rho = -0.0116\text{ kg}\cdot\text{m}^{-3}$, while the value $\Delta\rho = -0.0129\text{ kg}\cdot\text{m}^{-3}$ may be calculated from Eq. (14). The difference in $\Delta\rho$ values is small in absolute value, but it may be significant when quoting the density at $T=0$ to four decimal places, i.e., as $145.1397\text{ kg}\cdot\text{m}^{-3}$. Their calculation may be traced back to the specific-heat values of Ref. 6, which disagree with the present state equation by up to 7.7%, as seen in Fig. 3. This subject deserves review whenever the state equation is extended continuously to 1.344 K or above.

The temperature dependence of the sound velocity in the saturated liquid remains an enigma. Numerical evaluation from this state equation shows that the calculated sound velocity, from the calculated $\partial P/\partial\rho|_s$, decreases monotonically by $0.123\text{ m}\cdot\text{s}^{-1}$ or 0.052% as the temperature increases from 0 to 0.8 K at saturation pressure. The observed (first) sound velocity (Ref. 12, Table 3.3) increases by 0.02% from 0 to 0.6 K, with a subsequent decrease of 0.01% as the temperatures rises to 0.8 K. This observed maximum in sound velocity at about 0.6 K, although small in magnitude, has long been recognized as inconsistent with observed lattice

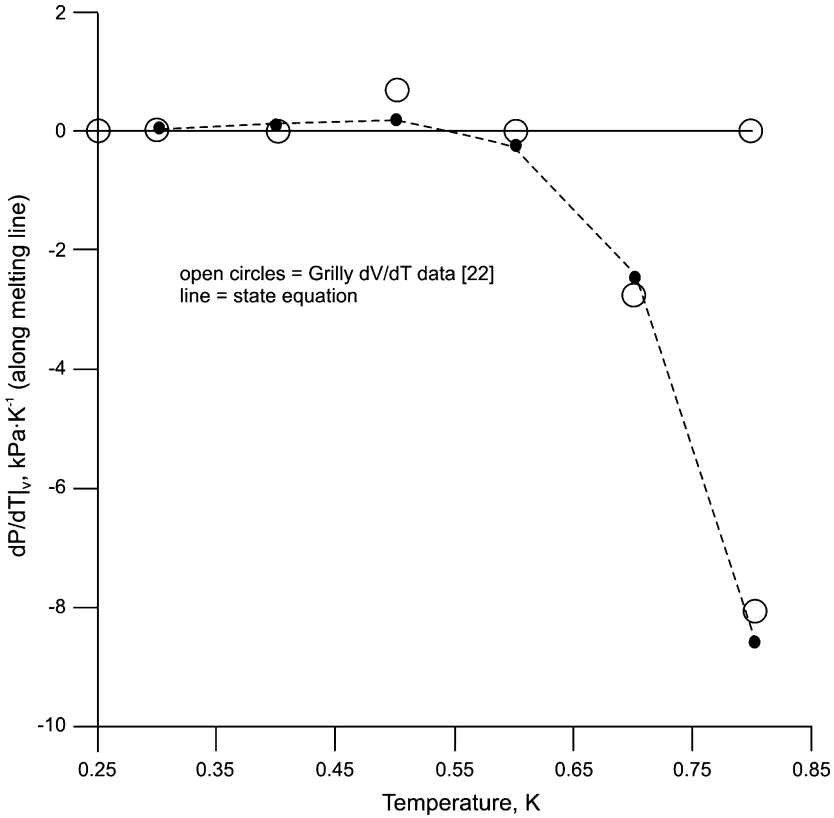


Fig. 6. Measured and state-equation values of $\partial P/\partial T|_v$ along the melting line as a function of temperature. Measured values were approaching the limits of experimental resolution, with 1 or 2 digit accuracy.

dynamics and specific-heat measurements. The present work offers no new insights to this quandary.

The phonon terms, Eq. (6) or (12), lead to a positive thermal expansivity, while the roton term, Eqs. (11) and (13), leads to a negative thermal expansivity. Thus, the bulk fluid expansivity is positive at lowest temperatures, becoming negative at higher temperatures and high pressures where the roton term begins to dominate. The predicted (P, T) locus of the line of zero expansivity varies from (2.532 MPa, 0.57 K) at the melting line to (0.902 MPa, 0.80 K) at the equation limit. No detailed experimental data exist to test the complete predicted locus. The locus intersects the saturation line at about 1.1 K [12].

The wide range of density dependences in the Helmholtz state equation, from ρ^{+3} to $\rho^{-8.6}$ is unique among fluid state equations. It is possible that such density exponent range may also be useful in state equations asymptotic to the lambda line. It is also possible that this variation may be found in low temperature helium-3 state equations. Both of these possibilities are currently under study.

7. EQUATIONS FOR $T > 0.8$ K

Essentially no experimental data exist between 0.8 and 1.2 K except along the saturation or melting lines. This temperature gap is a region of high dispersion and attenuation of sound velocities, describable in some sense as large phonon-roton interactions. The tabular data of Ref. 4 do bridge this gap, but their increasing disagreement with the present state equation between 0.5 and 0.8 K has already been noted. The equation of Ref. 21 includes a quasi-extrapolation into this gap region from the high-temperature side, but serious errors at the lower limit of 0.8 K have been noted above.

Above 1.2 K the mathematical description of thermodynamic properties is most successfully based on extended equations which are asymptotically correct at the lambda line but seemingly inconsistent with the mathematical form of Landau's Helmholtz equation. Also, the isothermal $P(\rho)$ data in an important reference publication [1] for temperatures from 1.2 K to the lambda line appears questionable [7, 23]. Spaceflight data [24] and recent theoretical advances [25] have fixed asymptotic lambda-line parameters at values differing measurably from those used in many prior studies, including Ref. 21.

I have come to the position that a thorough review and update of existing equations from 1.2 K to the lambda line should be completed prior to an interpolation equation through the data gap from 0.8 to 1.2 K.

8. CONCLUSION

Equation (15) utilizes relatively few terms to obtain consistency with all measured thermodynamic properties of He⁴ below 0.8 K. Individual terms are directly related to known theoretical components of the phonon and roton excitation spectrum. It incorporates a roton Helmholtz expression derived by Landau 60 years ago but little used since. In the limit of zero temperature, He⁴ is shown to have properties of a compressed phonon fluid, as measured by the Gruneisen parameter. The equation is unique among fluid state equations in that density exponents in the wide range from +3 to -8.6 are efficiently utilized. Use is made of the

empirical equation $c_1^3 \approx c_{10}^3 + bP$, where c_1 is the velocity of first sound, P is pressure, and c_{10}^3 and b are constants; this empiricism is found to apply also to other temperature ranges and to other fluids. The predicted variation in saturated liquid density from 0 to 0.8 K is about 11% greater than calculated from Ref. 17. This state equation forms a relatively reliable reference for possible future equations bridging the interval between 0.8 and 1.2 K where data are sparse.

9. APPENDIX A. $c^3(P)$

As a diversion from the goal of this paper, I have investigated the applicability of Eq. (1) to helium at higher temperatures, and to other fluids. Gammon [26] has reported very high accuracy sound-velocity measurements in He⁴ along 14 isotherms from -175 to $+150^\circ\text{C}$ with pressures to about 15 MPa. All of his individual isotherm data can be fitted to Eq. (1) with rms errors in c_1^3 ranging from 0.002% to 0.008%, with the ratio $b_2 P_{\text{max}}/b_1$ ranging from 0.2 at the lowest temperature to 0.015 at the highest temperature.

I also have least-squares fits of Eq. (1) to NIST standard reference data isotherms of N₂ up to 320 MPa at 115 K, CH₄ up to 180 MPa at 130 K, and H₂O up to 100 MPa at 400 K. Results are very close to a linear fit for each of these fluids above about 20 MPa. At lower pressures, measured sound velocities tend to drop below the linear fit. Note that these selected isotherms lie between the triple point and critical temperature for each fluid.

I suggest that Eq. (1) appears to be ubiquitously useful as a correlation tool in fluid properties studies, beyond its application in the present work. Further studies would be appropriate.

10. APPENDIX B. NUMERICAL COEFFICIENTS

Many reference publications have used molar rather than SI or cgs units. Units conversion is based on a He⁴ molecular weight of 4.0026.

Equation (5), (13), and (15) as written are based on SI units for A , P , ρ , and T . For numerical convenience Eq. (5) is rewritten here as

$$A_0(\rho) = 100(-a_{00}/r + a_{01} \log(r) + a_{02}r + a_{03}r^2 + a_{04}r^3 + A_{00})$$

where $r = 0.001\rho$. Then

$$\begin{aligned} a_{00} &= -62.40666, & a_{01} &= 1711.765, & a_{02} &= -18204.20, \\ a_{03} &= 30883.2, & a_{04} &= 6456.73, & A_{00} &= 4845.6707 \end{aligned}$$

The two terms in Eq. (13) are $\Delta_0 = 8.6023$ [K] and $m = -4.9795 \times 10^{-7}$ [K · Pa⁻¹]

The five coefficients in Eq. (15) are

$$a_1 = 0.0108487, \quad c_0 = 1.199942 \cdot 10^{-4},$$

$$c_k = -0.0017567, \quad f = 0.786846, \quad k = -8.5864$$

REFERENCES

1. J. Maynard, *Phys. Rev.* **B14**:3868 (1976).
2. M. S. Mongioli, *Phys. Rev.* **B48**:6276 (1993).
3. L. Landau, *J. Phys.* **5**:71 (1941).
4. L. Landau, *J. Phys.* **11**:91 (1947).
5. R. J. Donnelly and P. H. Roberts, *J. Low Temp. Phys.* **27**:687 (1977).
6. J. S. Brooks and R. J. Donnelly, *J. Phys. Chem. Ref. Data* **6**:51 (1977).
7. R. D. McCarty, *NBS Tech. Note 1029* (1980).
8. N. E. Phillips, C. G. Waterfield, and J. K. Hoffer, *Phys. Rev. Letters* **25**:1260 (1970).
9. N. E. Phillips, private communication (Univ. of California).
10. D. S. Greywall, *Phys. Rev.* **B18**:2127 (1978).
11. D. S. Greywall, *Phys. Rev.* **B21**:1329 (1979).
12. R. J. Donnelly and C. F. Barenghi, *J. Phys. Chem. Ref. Data* **27**:1217 (1998).
13. H. PrestonThomas, *Metrologia* **27**:3 (1990).
14. M. Durieux and R. L. Rusby, *Metrologia* **19**:67 (1983).
15. B. M. Abraham, Y. Eckstein, J. B. Ketterson, M. Kuchnir, and P. R. Roach, *Phys. Rev.* **A1**: 250 (1970); Erratum: *Phys. Rev.* **A2**:550 (1970).
16. H. J. Maris, *Phys. Rev. Lett.* **66**:45 (1991).
17. J. J. Niemela and R. J. Donnelly, *J. Low Temp. Phys.* **98**:1 (1995).
18. W. M. Whitney and C. E. Chase, *Phys. Rev.* **158**:200 (1967).
19. V. Arp, J. M. Persichetti, and G. B. Chen, *J. Fluids Eng.* **106**:193 (1984).
20. A. D. B. Woods, P. A. Hilton, R. Scherm, and W. G. Stirling, *J. Phys. C* **10**:45 (1977).
21. V. Arp, *J. Low Temp. Phys.* **79**:1 (1990).
22. E. R. Grilly and R. L. Mills, *Ann. Phys.* **18**:250 (1962).
23. V. Arp (to be published).
24. J. A. Lipa, D. R. Swanson, J. A. Nissen, T. C. P. Chui, and U. E. Israelsson, *Phys. Rev. Lett.* **76**:944 (1996).
25. M. Strosser, M. Monnigmann, and V. Dohm, *Physica B* **284-288**:41 (2000).
26. B. E. Gammon, *J. Chem. Phys.* **64**:2556 (1976).